Anal Bioanal Chem (2013) 405:8969–8980
DOI 10.1007/s00216-013-7129-1

REVIEW

Improving human health through understanding the complex structure of glucose polymers

Robert G. Gilbert · Alex C. Wu · Mitchell A. Sullivan · Gonzalo E. Sumarriva · Natascha Ersch · Jovin Hasjim

Received: 28 April 2013 / Revised: 1 June 2013 / Accepted: 6 June 2013 / Published online: 11 July 2013

Abstract Two highly branched glucose polymers with similar structures—starch and glycogen—have important relations to human health. Slowly digestible and resistant starches have desirable health benefits, including the prevention and alleviation of metabolic diseases and prevention of colon cancer. Glycogen is important in regulating the use of glucose in the body, and diabetic subjects have an anomaly in their glycogen structure compared with that in healthy subjects. This paper reviews the biosynthesis–structure–property relations of these polymers, showing that polymer characterization produces knowledge which can be useful in producing healthier foods and new drug targets aimed at improving glucose storage in diabetic patients. Examples include mathematical modeling to design starch with better nutritional values, the effects of amylose fine structures on starch digestibility, the structure of slowly digested starch collected from in vitro and in vivo digestion, and the mechanism of the formation of glycogen α particles from β particles in healthy subjects. A new method to overcome a current problem in the structural characterization of these polymers using field-flow fractionation is also given, through a technique to calibrate evaporative light scattering detection with starch.

Published in the topical collection *Separation and Characterization of Natural and Synthetic Macromolecules* with guest editors Albena Lederer and Peter J. Schoenmakers.

R. G. Gilbert · A. C. Wu · M. A. Sullivan
Tongji School of Pharmacy, Huazhong University of Science and Technology, Wuhan, Hubei 430030, China

R. G. Gilbert (✉) · A. C. Wu · M. A. Sullivan · G. E. Sumarriva · N. Ersch · J. Hasjim
Centre for Nutrition and Food Sciences, Queensland Alliance for Agriculture and Food Innovation, The University of Queensland, Brisbane QLD 4072, Australia
e-mail: b.gilbert@uq.edu.au

Keywords Health · Separations/theory · Field-flow fractionation · Foods/beverages · Polymers · Separations/instrumentation

Introduction

Starch and glycogen are both highly branched glucose homopolymers with linear bonds made up of α-(1⟶4) glycosidic linkages and branch points made up of α-(1⟶6) glycosidic linkages. These polymers have vital functions in biological systems. Starch is the energy reserve found in many parts of plants, including grain, fruits, leaves, stems, tubers, and roots, and is the primary energy source in human food and animal feed. Glycogen serves as a transient energy storage in animals, especially in muscle and liver cells, whose main function is to provide rapid energy to the cells when needed and to help maintain blood glucose homeostasis.

The structure of starch affects its digestibility, which in turn affects human health and nutrition. Starches that are quickly digested and absorbed rapidly increase blood glucose and insulin responses (hyperglycemia and hyperinsulinemia, respectively) after a meal and can promote metabolic diseases, including obesity and diabetes. On the other hand, those with slow digestion properties reduce the incidence of metabolic diseases and alleviate associated complications [1–3]. Furthermore, the portion of starch that resists digestion in the small intestine and reaches the colon (termed resistant starch, RS) is an important substrate for gut fermentation, the products of which include acetate, propionate and butanoate (butyrate). Butyrate has been shown to proliferate healthy colonocytes and suppress the development of cancer cells.

The structure of glycogen affects its breakdown in the human body. Because glycogen is the glucose storage polymer in animal muscle and liver cells, the body's abilities to synthesize glycogen and to release glucose when needed (such as in response to insulin and glucagon, respectively) are important to maintain a

stable level of blood glucose, avoiding episodes of hyperglycemia and hypoglycemia, which can be detrimental to human health. Type 2 diabetes is a disease related to the inability of the body to respond to insulin, and thus it is reasonable to suppose that glycogen is not synthesized properly when blood glucose levels are elevated. Indeed, it has recently been found that the liver glycogen from db/db mice (mutant mice which lack a gene for satiety and thus become obese and develop diabetes, thereby furnishing a laboratory animal model for type 2 diabetes) has a significantly different structure to that of healthy mice [4]. The understanding of glycogen synthesis in the body through the observation of the differences in the structure of glycogen between healthy and diabetic populations could identify which enzymatic processes of glycogen biosynthesis are missing in diabetic patients and allow the development of drugs to prevent or alleviate the symptoms of diabetes.

This paper examines the molecular structures of starch and glycogen and their implications in human health, especially the rapidly increasing rates of diabetes, obesity, and colorectal cancers. Techniques to accurately characterize the molecular structures are also discussed. Central to this is the paradigm that biosynthetic and biodegradative processes control the complex structure of these two branched polymers, while this structure in turn controls properties such as digestion rate. Characterization of this structure is therefore a key to significant human health challenges.

The material presented in this review focuses on innovations and results complementary to results summarized in two of our previous reviews related to this subject [5, 6].

Starch and glycogen structures and their relationships to human health

The structure of starch and glycogen can be divided into several levels (Fig. 1)

The lowest level (level 1) is the individual linear branches, where anhydroglucose units (or α-D-glucopyranosyl units, to use correct nomenclature) are linked by α-(1→4) glycosidic linkages. For glycogen, these branches are relatively short, with an average degree of polymerization (DP) of approximately 12. For starch, the branches fall into two categories: amylopectin, where the average DP is approximately 17–25, and amylose, where it is approximately 10^3–10^4.

Level 2 is the whole molecular structure, where the branches are linked by α-(1→6) glycosidic linkages. For glycogen, these linkages are essentially distributed randomly in a hyperbranched molecule, with an average molecular weight up to 10^7. Each glycogen molecule is termed a β particle. For starch, in amylopectin, the spacing between the α-(1→6) glycosidic linkages is controlled by debranching enzymes, which are absent (or at least much less important) in glycogen synthesis, such that the branches of amylopectin can undergo crystallization. Amylopectin is hyperbranched with an average molecular weight of approximately 10^7–10^8, i.e., there are a vast number of branches per amylopectin molecule. In amylose, the branches are randomly spaced, with only a few long branches per molecule; the average molecular weight is approximately 10^6. Glycogen, amylose, and amylopectin all have wide distributions of molecular weights and sizes in any given sample.

For starch, level 3 is the semicrystalline structure in which the amylopectin branches partially crystallize to form successive alternating crystalline–amorphous lamellae. Amylose molecules are present in either amorphous conformations or single helical complexes with lipid in native starch granules, both in the amorphous layers and interspersing among the amylopectin crystallites [7, 8]. Glycogen does not form a crystalline structure, because of the steric hindrance due to the high frequency of branching points. For the level 3 structure in glycogen, as seen particularly in liver cells, the β particles are joined (whether by intermolecular or chemical bonding is unclear, although information on this is emerging [9]), forming large entities known as α particles (or α rosettes), which can have diameters as large as 300 nm and molecular weights greater than 10^8.

For starch, higher structural levels comprise growth rings, granules, and the whole grain [10], and perhaps superhelices [11] and blocklets [12]. For glycogen, the higher structural levels comprise the arrangements of these molecules in animal cells, tissues, and organs.

These structural levels of starch are interrelated, and these multiple structural levels also control many functional properties of materials containing starch and glycogen. For example, starches with large proportions of shorter amylopectin branches (DP<25) have the A-type polymorphic crystalline structure (monoclinic unit cell) and show more pinholes on the surface and channels in the inside of starch granules, whereas those with larger proportions of long amylopectin branches (DP≥25) have the B-type polymorphic crystalline structure (hexagonal unit cell) and show a smooth surface and solid internal structure of starch granules [13, 14]. Starch digestibility is also highly correlated with the molecular structures. On the basis of the method of Englyst et al. [15], starch is grouped into three classes, which are rapidly digestible starch (RDS), slowly digestible starch (SDS), and RS. RDS is the starch digested in the first 20 min, which promotes metabolic diseases. On the other hand, SDS and RS are the starches digested between 20 and 120 min and that are not digested after 120 min, respectively, which can alleviate the symptoms of metabolic diseases [1–3]. Furthermore, RS is a good substrate for gut fermentation and has been shown to prevent the development of colon cancer. Uncooked native starch granule samples with higher proportions of short amylopectin branches (DP 6–12) have higher digestion rates, higher amounts of RDS, and lower amounts of RS than those with higher proportions of longer amylopectin

branches [16, 17]. However, these trends were not apparent after starch granules had been cooked beyond the gelatinization temperature. Greater amounts of amylose and extra-long amylopectin branches (DP>100) can also decrease the digestibility of both uncooked native starch granules and gelatinized starch [18]. This can be attributed to amylose, which intertwines among the amylopectin crystallites, maintains the integrity of the starch granule, and reduces the accessibility of enzymes into the granules. Amylose–lipid complexes, present in a greater amount with higher amylose content, can also restrict the swelling of starch granules during heating, thereby reducing the susceptibility of the starch to enzyme hydrolysis after heating [19, 20]. Furthermore, isolated branches of amylose and extra-long amylopectin branches can retrograde to highly ordered crystalline structures, which are highly resistant to enzyme hydrolysis, during the storage of gelatinized starch [21]. Retrograded amylose has been recognized as one type of RS. For glycogen, it has been recently found that the α particles are smaller and fewer in the livers of diabetic mice, whereas they are clearly observed in greater amounts of the livers from healthy mice, indicating the impaired ability of diabetic mice to form α particles [4]. It is therefore suggested that a drug enhancing the enzymatic biosynthesis of α particles in the liver might be able to alleviate the symptoms of diabetes.

Various characterization techniques are now discussed.

Level 1: *Individual branches*

There are three techniques that have been commonly used to analyze the chain-length distribution (CLD) of the branches in starch and glycogen molecules. These are fluorophore-assisted carbohydrate electrophoresis (FACE), high-performance anion exchange chromatography (HPAEC), and size exclusion chromatography (SEC). The CLD analysis is carried out after the starch or glycogen molecules have been treated with isoamylase, a debranching enzyme, which specifically and quantitatively cleaves the α-(1⟶6) glycosidic bonds, leaving the linear chains of α-(1⟶4) glycosidic bonds intact.

FACE [22, 23] separates linear chains of debranched starch or glycogen on the basis of the mass-to-charge ratio after each chain has been labeled with a negatively charged fluorescent dye (the commonest being 8-aminopyrene-1,3,6-trisulfonic acid, APTS) at the reducing end. It has been shown that the labeling with APTS is quantitative up to degree of polymerization of approximately 135 [23]. Because there is only one charged group per molecule, the different sizes of the linear chains create different mass-to-charge ratios, allowing the separation by FACE based on chain length with baseline resolution between the chains of different DPs. Detection uses fluorescence. Similarly, HPAEC, usually equipped with pulsed amperometric detection (PAD) [24, 25], can be used to obtain CLDs with baseline resolution but without needing a fluorophore: the molecules are separated on the basis of the number of alkoxide groups at alkaline pH, giving a separation based on monomer size (one anhydroglucose monomer has three alkoxide groups at alkaline pH). The signal intensity is, however, mass-dependent, making it less accurate than FACE. The mass dependence of the PAD signal intensity can be corrected by hydrolyzing the separated molecules into monomer, i.e., glucose, using an on-line amyloglucosidase reactor column [26], but this is very laborious. For both techniques, there is baseline separation of the signal between oligomers of different

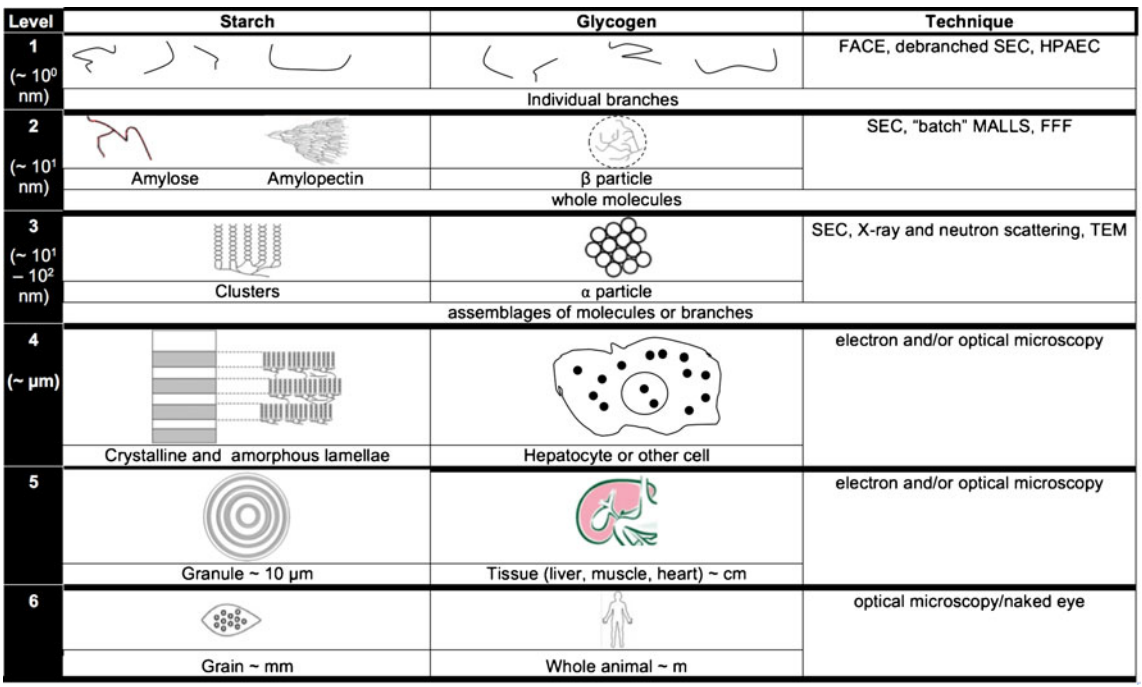

Fig. 1 The structural levels of starch and glycogen

DPs, and so calibration is simply by adding an α-(1⟶4)-linked glucose marker of known DP. Owing to the low sensitivity of the detectors towards larger molecules, the CLDs obtained are confined to a maximum DP of approximately 100 for FACE and somewhat less for HPAEC, and hence can give information on glycogen branches and almost all amylopectin branches, but not amylose branches and extra-long amylopectin branches.

SEC, on the other hand, is able to provide the whole CLD of both amylopectin and amylose branches as well as glycogen branches, and the signal with differential refractive index (DRI) detection is simply proportional to mass. SEC separates molecules on the basis of hydrodynamic size, which is directly related to the molecular size for linear polymers such as debranched starch and glycogen. Thus DRI detection is sufficient for the analysis of the CLD of starch or glycogen. Furthermore, the molecular sizes of the linear molecules from debranched glycogen, amylopectin, and amylose are within the separation ranges of readily available SEC columns, and these molecules have almost 100 % recovery owing to their small molecular sizes. The relationship between SEC elution volume or time and hydrodynamic size (i.e., hydrodynamic volume or radius) can be obtained using narrowly distributed standards, such as dextrans and pullulans, with known molecular weights that can be converted to hydrodynamic size, and the DP of the separated linear molecules is obtained from the hydrodynamic volume or radius using the Mark–Houwink equation (see, e.g., [27] for details of how this standard technique is applied in practice). However, all SEC systems suffer from band broadening; it is not possible to obtain baseline resolution, and the quantitative form of the distribution requires deconvolution (which is a complex process [28–30] and not yet able to be implemented for debranched starch and glycogen on a routine basis). Thus the fine details of a CLD such as small shoulders, easily obtained by FACE and HPAEC, are not readily apparent in SEC.

The CLD of starch molecules obtained using SEC can also be used to determine the amylose content of starch with amylose content less than 40 % as the ratio of the area under the curve (AUC) of amylose branches (e.g., DP>100) to the AUC of the whole CLD [31]. For high-amylose starch (>40 % amylose content), there is substantial overlapping between the AUC of amylose and amylopectin branches in the CLD obtained by SEC, and thus the estimated amylose content is less accurate. A two-dimensional SEC distribution [31], discussed below, allows a better separation between amylose and amylopectin populations, and thus gives a more accurate amylose content of high-amylose starch; however, the technique is very laborious.

The average degree of branching can be obtained using ^{1}H NMR spectroscopy from whole starch or glycogen molecules (not from debranched starch or glycogen) [32–34]. With improved methodology [33], this average can be obtained to a greater accuracy than by averaging the whole CLD.

Level 2: *Whole molecular structure*

Several techniques exist for characterizing this structural level. Multi-angle laser light scattering (MALLS) (without size separation) gives the weight-average molar mass, $\overline{M}_w$, and z-average radius of gyration, Rg,z. Various size-separation techniques can be used to obtain various size distributions. It is essential to be aware that all size-separation techniques are exactly that: they separate by size, not by molecular weight. Although there is a unique relation between size and molecular weight for linear polymers, no such relation exists for (complex) branched polymers. Except for mass-spectrometric methods, which are confined to relatively low molecular weights, it is therefore impossible to obtain a molecular weight distribution of a branched polymer by any separation technique (although unfortunately some manufacturers' software report a molecular weight, but this is obtained from the data with the implicit assumption that the polymer is linear, and thus is incorrect; if there is MALLS detection, then the molecular weight axis is actually $\overline{M}_w$). The three size-separation techniques considered here are SEC, asymmetric-flow field-flow fractionation (AF4) [35], and hydrodynamic chromatography (HDC) [36]. All have various advantages and disadvantages. For all techniques, a number of detectors can (and should) be used: DRI, which is mass-sensitive; MALLS, which measures $\overline{M}_w$ and Rg,z; and viscometry, which (together with DRI detection) measures intrinsic viscosity and hence (through the universal calibration assumption [37, 38]) the number distribution [39, 40]. The separation parameter for any size-separation technique is, by IUPAC definition [41], always termed hydrodynamic volume, V_h (or the corresponding hydrodynamic radius, R_h); however, the relation of this quantity to molecular properties varies with the separation technique. The mass distribution is denoted by $w(\log V_h)$, and is the weight of molecules in the logarithmic increment of hydrodynamic volume, $\mathrm{d}(\log V_h)$. The number distribution is denoted by $N(V_h)$ (the number of molecules in the increment of hydrodynamic volume, $\mathrm{d}V_h$), and similarly for $\overline{M}_w(V_h)$ and $R_{g,z}(V_h)$.

For SEC, the size-separation parameter, V_h, is proportional to the product of the weight average of the intrinsic viscosity and the number average of the molecular weight [38]. For AF4, the separation parameter is the size inferred using the Stokes–Einstein relation from the center-of-mass diffusion coefficient [35]. The size-separation parameter for HDC of complex branched molecules has not been yet rigorously established. All size-separation techniques require calibration: for example, with SEC this is through the use of linear standards with known hydrodynamic volume together with the universal calibration assumption. This assumption is that the elution time is solely governed by V_h, and not any other aspect of polymer structure, such as composition.

For all size-separation techniques, it is necessary to dissolve the analyte completely and with molecular separation, without aggregation or molecular degradation. The best verified solvent for this purpose is dimethyl sulfoxide (DMSO), sometimes with a small amount of water or lithium salt, such as LiBr (see, e.g., [42, 43]). Some workers then redissolve the starch in an aqueous medium before analysis (e.g., [44]). Whether this type of technique results in any degradation or aggregation is currently under investigation by an IUPAC working party [45]. The corresponding procedure for glycogen is quite complex but verified [46].

SEC is useful for characterization of starch and glycogen, but it has some limitations. For example, the size of the largest commercially available DMSO-soluble standard is much smaller than the size of amylopectin molecules (the R_h values obtained by SEC in DMSO solution with 0.5 % w/w LiBr are approximately 50 nm and nominally up to 5,000 nm, respectively—the large upper bound being almost assuredly an artifact from the extreme extrapolation used to obtain this figure [47]), and extrapolation of the universal calibration curve is prone to high inaccuracy [27]. Furthermore, owing to its large molecular size, whole amylopectin molecules inevitably suffer from shear scission [47] and low recovery during SEC separation. In addition, the size of whole amylopectin molecules often lies outside the optimal separation ranges of many SEC columns, and thus the separation is greatly affected by sample concentration and band broadening [27]. Unfortunately, there are quite a few papers in the literature which present data such as $\overline{M}_w$ obtained using SEC on amylopectin which have not taken shear scission into account, and any conclusions reached from such results contain this major experimental artifact. Whole amylose and glycogen molecules are smaller than whole amylopectin molecules; hence they suffer minimal shear scission, and the separation of these molecules is essentially within the optimal separation range of SEC column and has almost 100 % recovery [33].

The $\overline{M}_w$ and $R_{g,z}$ of whole starch and glycogen molecules are obtained using a MALLS detector without size separation, which avoids the problem of shear scission. The $\overline{M}_w$ and $R_{g,z}$ obtained by MALLS are sensitive towards larger molecules. Data fitting for MALLS is usually carried out using a Berry plot for large molecules, such as amylopectin, and a Zimm plot for smaller molecules, such as amylose and glycogen. Because of the high sensitivity of light scattering to particle size (the signal being proportional to the sixth power of radius), the data are very prone to problems with reproducibility. For this reason, it is essential to replicate the MALLS measurements, e.g., on different days with fresh sample.

In addition to detection with MALLS (which is static light scattering), dynamic light scattering (photon correlation spectroscopy) can also be used (e.g., [44]), although considerable care should be taken in its implementation, as this technique is even more prone to irreproducibility than is MALLS. It is also noted that any type of detector can in principle be used off-line by collecting samples after size separation which are then characterized as desired, e.g., by NMR or small-angle X-ray scattering.

Size separation of starch by HDC shows poor amylose–amylopectin resolution and, similar to SEC, shear scission of amylopectin molecules [48].

Two-dimensional size distributions Two-dimensional distribution, where one dimension is the CLD or SEC weight distribution of individual linear branches and the other dimension is the SEC weight distribution of whole molecules, can provide more detailed structural information of starch and glycogen molecules [49, 50]. This includes the presence of hybrid components, especially intermediate components which are highly branched like amylopectin, but with molecular size similar to amylose, and also amylopectin molecules with extra-long branches. The 2D distribution is obtained by collecting the fractions from the SEC separation of whole molecules, debranching each fraction with isoamylase, and reanalyzing each debranched fraction using SEC: the technique is thus of the type SEC×SEC.

Amylose content The amylose content of starch can be determined on the basis of its structure or properties. From the structure, the SEC weight distribution of individual branches (or CLD) as mentioned above can give quite accurate amylose content of starch with amylose content less than 40 %, which is estimated from the AUC of amylose branches to the AUC of the whole CLD [31]. The SEC weight distribution of whole molecules, however, gives a less accurate estimate than the CLD and 2D SEC distribution because of the limitations of SEC when analyzing whole amylopectin molecules, including shear scission and low recovery, as mentioned above. Furthermore, the SEC weight distribution of whole molecules cannot differentiate between intermediate components and amylose, as they have similar molecular size, and thus may overestimate the amylose content of starch containing substantial amounts of intermediate components, such as high-amylose maize starch. Because the 2D distribution gives clear separation between amylose and amylopectin populations, it can also be used to accurately estimate the amylose content of starch [31, 49], but it is extremely laborious to implement.

Amylose content can be estimated from the ability of amylose to form complexes with iodine and lipids and from the affinity of concanavalin A to precipitated amylopectin. Amylose–iodine complexes can be determined colorimetrically or potentiometrically [13, 51], whereas the amylose–lipid complex is determined using differential scanning calorimetry [52]. The method using concanavalin A is normally followed by enzymatic hydrolysis of amylose, which remains

in the supernatant, to glucose for colorimetric detection using enzymes including glucose oxidase and peroxidase [53]. Because these methods do not directly measure the amount of amylose molecules, the analyses need to be handled with caution. For example, the complete removal of endogenous lipids in starch granules is critical, as they can inhibit the complex formation between amylose and iodine or added lipid. In addition, amylopectin can bind with iodine to a lesser extent, which can affect the accuracy of the results.

Glycogen α and β particles The techniques can be used to differentiate the glycogen α and β particles include SEC, light scattering analysis without size separation (such as MALLS or backwards scattering), and transmission electron microscopy. SEC is currently the best method [4, 9, 54], especially as the size of glycogen is significantly smaller than that of amylopectin, so the size separation of glycogen particles is less affected by problems such as shear scission and low recovery.

Examples

A recent review [6] included discussion of two interesting structure–structure and structure–property relations in starch, namely between fine structure (level 1) and crystalline structure (level 3) [55], and between fine structure and digestion rate [56]. The latter relation showed for the first time that amylose fine structure significantly affects starch digestion rates of cooked rice grains, which can be better understood as follows. Although many studies have reported that larger amounts of long and extra-long amylopectin branches and greater amylose content decrease the digestibility of starch, any effects of amylose molecular structure on starch digestibility are not yet well established. This could be due to a general belief that there is not much variety in amylose structure among starches from different botanical origins, as amylose molecules are only lightly branched, and are synthesized mainly by only one enzyme, namely granule-bound starch synthase. Thus it is generally thought that amylose content is sufficient to understand the effects of amylose on starch physicochemical properties. However, it has been shown (e.g., [56, 57]) that not only are the structures at levels 1 and 2 significantly different among different varieties, but also the amylose CLD shows more than one population, suggesting that more than one enzymatic processes is involved in synthesizing amylose in a plant. The first study using 2D SEC analysis revealed that amylose molecules of small hydrodynamic volume have a greater amount of longer branches than large amylose molecules [49], suggesting that larger amylose molecules have more branching points and shorter average branch chain-length.

Further examples are given below.

Example 1: *Developing plants containing starch with improved nutritional value*

The CLD of the branches of starch molecules is governed by biosynthetic processes in living plants, which involve the concerted actions of multiple enzyme types and isoforms. The processes in different organs have significant differences (e.g., endosperms vs. leaves). However, in all plants, the core biosynthetic enzymes involved are as follows. ADP-glucose pyrophosphorylase (AGPase) produces the soluble substrate, ADP-glucose, for starch synthesis. Starch synthases (SSs) catalyze elongation of glucan chains by adding ADP-glucose to pre-existing glucan chains via α-(1⟶4) glycosidic linkages. Starch branching enzymes (SBEs) are responsible for cleaving glucan chains and transferring cleaved chains to other chains via α-(1⟶6) glycosidic linkages to create new branches. Debranching enzymes (DBE), both isoamylase and pullulanase types, hydrolyze α-(1⟶6) glycosidic linkages, thereby removing branches.

CLDs are used here to understand the biosynthetic pathway of starch, by comparing the CLDs from different species or varieties. An important issue is how to use these CLD data quantitatively. The empirical approach commonly used for treating these CLDs is to convert them into "difference plots", i.e., the differences between a series of normalized CLDs compared to some reference distribution (e.g., various varieties compared to one chosen reference variety). This is often used to infer the roles of the biosynthetic enzymes in determining the fine structure of starch, amylopectin in particular. This procedure is empirical, without any biosynthetic basis.

A non-empirical procedure to use CLD data is the following. Modeling of starch CLDs has led to new understanding of the starch biosynthetic pathway in cereal endosperms [58, 59]. This modeling is developed analogously to that used in synthetic polymers. The model considers the core biosynthetic enzymes, and gives excellent agreement with a wide range of CLDs in endosperms. Despite the complexity in starch biosynthetic pathways, the CLD can be conveniently presented through this modeling to focus attention on the key determinants of starch structure.

The model allows CLDs to be parameterized by a small number of biosynthesis-based parameters. It has been found (e.g., [55]) that this new parameterization provides an improved tool for a statistical identification of structurally important characteristics of a starch, arising from the underlying biosynthesis, with regard to properties such as crystallinity and digestibility. Code for implementing this is publicly available [60]. Furthermore, using this mathematical modeling, it is possible to predict which enzyme to alter to produce starches with better nutritional value, such as those with longer amylopectin branches.

Example 2: *New detection system for AF4 with starch*

Size separation by AF4 avoids shear scission, because the shear is much gentler. This is a great advantage over SEC, and opens a way to accurate characterization of whole amylopectin (level 2) structure. However, there are also disadvantages. Some excellent work has been done using the asymmetric-flow variant, AF4, for starch in aqueous solvents following initial dissolution in DMSO (e.g., [44, 61]); however, the question of complete molecular dissolution without aggregation and molecular degradation has not yet been settled for this dissolution method. A viscometric detector cannot be used for AF4 because of the interference from the flow system. It is also essential to ensure that separation is indeed by size ("Brownian mode") and not by something else, such as "steric/hyperlayer mode" when the separation parameter is no longer some measure of size [35]. The DRI signal is proportional to both mass and the differential refractive index dn/dc (c=polymer concentration, n=-refractive index), which among other factors is dependent on solvent system. For amylopectin in a DMSO-based solvent, dn/dc is very small (whereas it is significantly larger in aqueous solvents, where this particular problem does not exist), and under the conditions where elution is Brownian, the concentration of size-separated analyte is so low that the DRI signal gives an unacceptable signal-to-noise ratio [5].

We now present a novel way to overcome the problem of poor signal-to-noise ratio with AF4 for amylopectin in DMSO. Evaporative light scattering (ELS) detection is considerably more sensitive than DRI, but the signal is not a simple function of sample mass. However, we find here that it is possible to construct a calibration curve relating signal to mass, but the calibration varies with starch molecular size.

Three samples of amylopectin were tested as follows. The first was an unmodified waxy (ca. 100 % amylopectin) maize starch (Mazaca). Two further samples were degraded amylopectin (denoted 105.40.70 and 105.40.130) prepared from the waxy maize starch (by Ms. Ming Li) using extrusion in the presence of glycerol as plasticizer. The extrusion process reduced the overall molecular size significantly, but would not have changed the branching structure of starch. Extrusion probably breaks bonds in a random fashion throughout the molecule. The resulting size reduction will be commensurate with (although somewhat smaller than) that produced by scission events which, on average, halve the hydrodynamic volume of an amylopectin molecule. However, but there are such a vast number of bonds that even a large size reduction will have a miniscule effect on branching structure (unless the process were so extreme as to reduce the parent molecules to oligomers).

The ELS detector used in this study was PL-ELS 1000 (PSS, Mainz, Germany). A range of concentrations for each sample, dissolved in DMSO, was then tested with this detector. It was found that the signal for higher concentrations varied in time, i.e., rising to a maximum, decreasing, and then gradually increasing again. This last rise is attributed to build-up of degradation products in the system. The signals at the minimum (after about 1 min) of different concentrations were plotted for each sample to produce the dependences of signal on concentration. The results are shown in Fig. 2. It is apparent that, for samples of a given average size (i.e., obtained from given extrusion conditions), there is a monotonic relationship between signal and concentration; however, this relationship depends on the molecular size of the sample.

The origin of this effect is apparent when one considers how ELS works. The eluent stream enters the detector into an evaporation chamber and passes through a heated nebulizer in the presence of a nitrogen gas stream. This shears the droplets and begins to atomize the solution into a relatively uniform droplet dispersion. The atomized spray is carried by the nitrogen gas to the evaporation chamber, where the solvent evaporates from the atomized spray and dry particle plumes remain. This process is assisted by a diffuser, which functions as a heat exchanger and prevents particles from sticking together, while transporting them to the scattering chamber. Light passes through the instrument perpendicular to the direction of gas flow. When a non-volatile sample particle is present, the "cloud" passes through the light path and scatters the beam. This scattered light enters the optical aperture at right angles to the light source and generates a signal response in real time at the photodiode. The stronger the scattered light, the stronger the signal, the intensity of which depends on solute concentration and the particle size distribution. It is apparent that the size of the molecules in the eluent can affect the signal, especially through the particle size distribution.

What these results show is that ELS detection can be used as a mass-sensitive detector, e.g., in AF4 with a DMSO-based eluent, provided one can calibrate both concentration and molecular size. The molecular size can be obtained either on-line or off-line using MALLS, and the concentration by using calibrants that have been previously size-

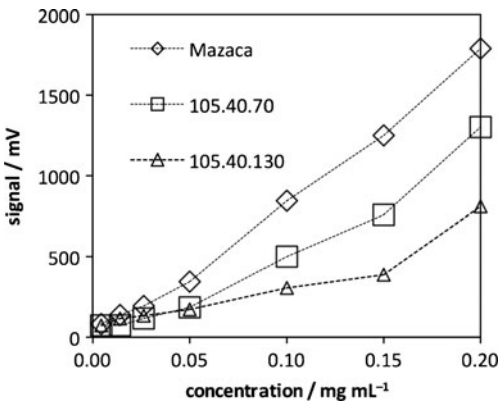

Fig. 2 ELS signal as a function of concentration for various starch samples

separated, which is not a difficult task with AF4 because significant amounts of eluted sample can be obtained.

This then is a method to overcome the problem of the poor signal-to-noise ratio when using DRI detection in AF4 with DMSO, by using instead ELS detection with the new technique.

Example 3: *Time evolution of starch structure during in vitro and in vivo digestion*

Starches with slow digestion and/or enzyme resistance properties are desirable because of their health benefits such as the prevention and alleviation of metabolic diseases. RS can also prevent colon cancer. As described above, the structure of starch can greatly affect its digestibility. Several structures have been associated with RS, which is divided into five groups:

RS type 1: physically inaccessible starch, such as those embedded in protein and cell wall matrices in cereal grain or coarse ground meal
RS type 2: native B- and some C-type polymorphic starch granules
RS type 3: retrograded amylose
RS type 4: chemically modified or cross-linked starch
RS type 5: amylose–lipid complex

The structure of SDS is not well understood because it varies greatly between native starch granules and gelatinized starch. Normal cooking processes tend to gelatinize starch, increasing the RDS content and decreasing both SDS and RS contents [62–64]. The SDS contents of cooked maize and rice flours after overnight storage at 4 °C are negatively correlated with their RDS contents [65, 66]. Furthermore, studies on chemical and enzymatic modification of starch structures showed that SDS increased with RS, whereas RDS decreased [63, 67]. On the other hand, studies using physical modification of native starch granules, such as annealing and heat-moisture treatment, showed that RDS and SDS decreased by increasing RS and vice versa [64, 68, 69]. Starch structure can change during digestion, which can contribute to the slow digestion and enzyme-resistance properties [70, 71].

Witt et al. [72] investigated starch structural changes during in vitro digestion using extruded starch (essentially a model for pasta) from waxy, normal, and high-amylose maize starches. The SEC weight distribution of whole (fully branched) starch molecules revealed that amylose and amylopectin molecules were quickly digested to smaller dextrins with R_h of approximately 2–3 nm in DMSO solution with 0.5 % w/w LiBr. Only the peaks of these dextrins were visible in the SEC weight distributions of non-waxy extruded starches after 24 h in vitro digestion and the amount was larger with higher amylose content, although the amount decreased with digestion time, showing an "all or none" mechanism, whereby each dextrin molecule was digested to completion before another dextrin molecule was digested. The extruded waxy maize starch, on the other hand, was almost completely digested after 24 h digestion. The CLD also showed the appearance of a dominant population of branches with R_h of approximately 2–3 nm (DP ca. 50) after in vitro digestion, indicating that most of these slowly digested dextrins were linear. Jane and Robyt [73] reported that the DP of retrograded amylose after digestion with α-amylase from *Bacillus subtilis* has a DP of 50. It seems that the linear dextrins produced during digestion can crystallize into a highly ordered structure that is not easily accessible by enzyme.

Another study compared the structural changes of native normal maize starch granules during in vitro and in vivo digestion [74]. The in vivo digesta were collected from pig small intestine. The structural changes of native normal maize starch granules in the in vitro digesta were similar to those of extruded starch previously reported [72], where amylose and amylopectin molecules were quickly digested to smaller dextrins with R_h of approximately 2–3 nm, and only the peak of these small dextrins was visible in the SEC distribution after 24 h in vitro digestion. The amylose and amylopectin population in the SEC weight distributions of whole starch molecules from the in vivo digesta, however, mostly remained unchanged in the upper half of the small intestine, whereas the population of the small dextrins with R_h of approximately 2–3 nm became dominant in the lower half of the small intestine, along with smaller amounts of larger molecules. The peak of the small dextrins with R_h of approximately 2–3 nm also appeared in the SEC weight distributions of the individual branches of starch molecules (or enzymatically debranched starch) in the digesta after 24 h in vitro digestion and in the digesta from the lower half of small intestine (in vivo digestion), although the former only had one peak, whereas the latter had at most two additional smaller peaks at larger R_h. The results indicate that small dextrins are linear, similar to those from extruded non-waxy starches [72]. However, the in vitro digestion seems to be more homogenous than the in vivo digestion, probably owing to some enzymes being only present in the intestinal lumen and others on the brush border of the intestinal wall in the in vivo system, whereas all enzymes in the in vitro system are soluble in the solution. Furthermore, although native normal maize starch granules have been suggested as a source of SDS from an in vitro method [75], they were shown to be almost completely digested before reaching the lower half of the pig small intestine, indicating that current in vitro methods need a validation from the in vivo method in assessing the accurate nutritional value of starch.

Example 4: *Structure of glycogen in healthy and diabetic mice*

The db/db mouse suffers from obesity, hyperglycemia, transient hyperinsulinemia and hyperglucagonemia, making it a useful model for type 2 diabetes [76–78]. These symptoms,

which are only present in db homozygotes, are caused by a point mutation in the leptin receptor gene [79].

SEC has recently been used to compare the weight distributions of healthy (db/+ and +/+) and diabetic (db/db) mouse liver glycogen [4]. The results in Fig. 3 show that db/db mice are unable to form as many large α particles as healthy mice, with their glycogen distributions comprising mainly β particles and some small α particles. This result is consistent with previous data obtained using sucrose density centrifugation, which suggested that there were less dense glycogen molecules in db/db mice [80]. The CLD of debranched glycogen from db/db and db/+ mice suggested that the glycogen from diabetic mice has a slightly smaller proportion of longer branches than that from healthy mice [4]. This is consistent with past studies that reported the average chain length of db/db mice to be smaller than that of healthy mice [80].

Given the statistically significant (and qualitatively striking) difference between the structure of liver glycogen from healthy and db/db mice, a number of questions have become increasingly relevant. What is the expected physiological impact of having a distribution of smaller liver-glycogen molecules? What holds α particles together and why is this impaired in db/db mice? Is this effect seen in other models of type 2 diabetes?

It has been suggested [4, 78] that smaller glycogen molecules, with a greater surface area to volume ratio (and thus more exposed chain ends per monomer unit) are able to degrade faster than the larger α particles. This is conceivably the reason why evolution has favored the formation of large α particles in the liver, where glucose release needs to be slow and tightly controlled, as opposed to the smaller β particles found in muscle tissue where glycogen needs to be broken down rapidly during exercise. It is therefore possible that poor glucose control is at the very least exacerbated in db/db mice by impaired α particle formation.

The question of what holds α particles together has proven to be difficult to resolve, with a number of past studies coming to conflicting conclusions. The possibility of hydrogen bonding has been consistently negated by experimental evidence [9, 54, 81], suggesting a covalent link. Whilst the disulfide-disrupting reagent 2-mercaptoethanol appeared to cause α particles to break down, it appears [4, 82] that this is an artifact. Another study also used 2-mercaptoethanol and iodoacetamide and reported no change in the size of liver glycogen [83]. The authors suggested that the link between β particles may just be an α-(1→4) glycosidic linkage, the same bond used to connect glucose units in a glycogen chain.

Recently light was shed on this issue using one of the characterization techniques discussed in the present paper. SEC was used to obtain the weight distributions of glycogen at different times after being exposed to a relatively low pH (ca. 3.5) [4]. Whilst it is well known that acid can hydrolyze glycogen [81, 84], only when these semiquantitative distributions were obtained did it become obvious that the bonds holding α particles together were degraded much faster by acid hydrolysis than the normal glycosidic linkages in glycogen. This was consistent with past sucrose density centrifugation data [85]. Furthermore, it was shown in this recent SEC study that, even at neutral pH, α particles can be degraded into β particles. The degradation rates of α particles to β particles in both acidic and neutral pHs were found to be consistent with the hydrolysis of protein [86, 87]: the "glue" whereby the β particles in α particles are held together is probably some type of protein.

One major implication of α particles being held together by protein (as suggested although not proven by experiment), as opposed to just α-(1→4) or α-(1→6) glycosidic linkages, is a new potential target for clinical intervention. Approximately half of the orally dosed drugs used clinically are small molecules that inhibit the action of enzymes [88, 89]. Therefore any enzyme that may be linked to impaired α particle formation (or increased α particle degradation) may potentially become a new drug target for inhibition. If a "glue" protein is found, a new drug that upregulates this protein to increase the synthesis rate and the molecular size of α particles becomes a possible intervention for diabetic patients.

Whilst the analysis of glycogen structure using SEC and FACE to better understand the role glycogen in diabetes is

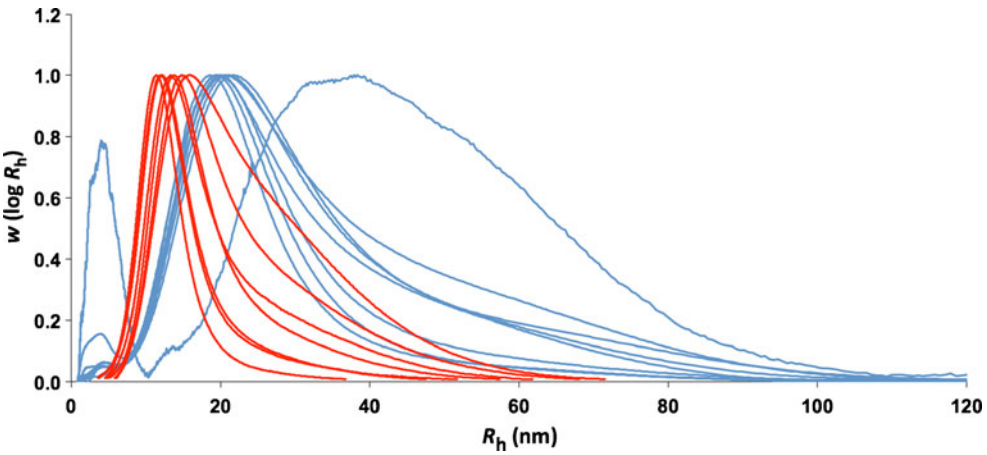

Fig. 3 SEC weight distributions of glycogen from livers of healthy (*blue*) and diabetic (db/db; *red*) mice. Those for db/db mice are reprocessed from earlier work [4]; those for healthy mice are new data for livers from healthy mice fed ad lib and all sacrificed at the same time (9–10 p.m.). The peaks sometimes seen at very small molecular sizes are artifacts due to residues of unidentified components not removed by the extraction procedure

still in its infancy, the results obtained thus far have refueled a number of questions regarding α particle formation and degradation. These techniques will help in exploring the full potential of manipulating the glycogen cycle as a clinical strategy in diabetes management.

Example 5: *No effects*

We now summarize two recent results showing that sometimes the fact that there are *no* effects of starch structures by genetic manipulations or alteration in growth conditions is important.

The first concerns dwarf varieties of grain-producing plants. The advent of dwarf varieties (the Green Revolution) had a revolutionary effect on agricultural productivity in the developed and developing world: indeed, in the developing world, this removed the looming specter of mass starvation. A recent study examined the effects of the dwarfing genes on starch quality: is the starch structure significantly changed in dwarf varieties compared with wild-type or tall varieties? This is a separate question from the over-riding societal importance of these varieties: if there were to be a significant change in starch structure, this might have an effect on the nutritional value of these crops (as exemplified in the discussions above on the effects of starch structure on digestibility). It was found [90] that in actuality there was no significant structural effect, a result which can be readily rationalized in terms of the underlying genetics.

Another example concerns the effects of growth temperature on starch molecular structure (levels 1 and 2) [91] in sorghum. It was found that there were some changes in the CLD of debranched starch (level 1), showing that some enzymatic activities depend on growth temperature. However, for the whole molecular structure (level 2), it was found that total molecular size and weight-average molecular weight (obtained by MALLS) did not appear to be sensitive to growth temperature. This surprising result can be rationalized by considering what controls the cessation of growth of a whole starch molecule (rather than of individual branches). The result suggests that the hypothesis that the cessation event is diurnal in nature is incorrect. The data are, however, consistent with the hypothesis that overall growth stoppage occurs as the outer part of the molecule becomes inaccessible to biosynthetic enzymes, probably because the outer branches become very dense and so impede access.

Conclusions and outlook

The full structural characterization of starch and glycogen is a challenge for separation scientists. This paper reviews the best current methods for this characterization and exemplifies how this can lead to new knowledge of importance to human health.

Starch and glycogen have very complex multi-scale structures, with up to six separate structural levels, from nanometers to millimeters, able to be identified. This critical review looks at the lower levels: those of the individual branches, the whole branched molecule, and (for glycogen) the binding of these into clusters termed α particles (or α rosettes). These structural levels are characterized by a range of techniques, of which the best are as follows. (a) For individual branches (the CLD), fluorophore-assisted capillary electrophoresis for individual branches containing fewer than approximately 100 monomer units (glycogen and amylopectin branches), and size-exclusion chromatography for longer branches (amylose branches and longer amylopectin branches). The amylose-to-amylopectin ratio can be found from the SEC CLD; colorimetric methods are less precise. The branching fraction can be found from the number average of the CLD, but more accurately by NMR. (b) For fully branched molecules, it is first essential to use an extraction and dissolution method which fully and molecularly dissolves the polysaccharide without degradation; for starch, it is generally agreed that this procedure involves initial dissolution in DMSO, and a complex but reliable procedure has been established for glycogen. The dissolved analyte is best characterized using multiple-detection size separation with either SEC or field-flow fractionation with multiple detection (DRI, MALLS, and viscometric being the most common). It is essential to avoid a common error in the literature that SEC and AF4 separate by molecular weight; that is not the case, because size-separation techniques separate by size. For complex branched polymers such as starch and glycogen, it is impossible to obtain an actual molecular weight distribution; the best that can be obtained (using triple detection) is the size distribution of weight- and number-average molecular weights. Both SEC and AF4 have significant drawbacks. Shear scission cannot be avoided in SEC for amylopectin. Unfortunately many papers in the literature have reported data without taking this into account, whence any conclusions from such data are unreliable. For AF4 , although shear scission is not a problem, it is not yet clear whether or not use of a water-based eluent system following initial DMSO-based dissolution causes sample loss or association. On the other hand, DMSO as an eluent with AF4 cannot give adequate signal-to-noise ratios with mass-sensitive (differential refractive index) detection under conditions where separation is by size, i.e., one can tell one has size separation, but no idea what the concentration is. The results from an IUPAC working party examining the DMSO/water dissolution system used by a number of high-quality laboratories should answer the question of the validity of this aqueous technique, which would overcome the detection problems.

We report here a potential solution to this problem using a more sensitive detector with AF4 , namely ELS (evaporative light scattering), using a special calibration method which

overcomes the difficulty that the signal of this detector is not a simple function of analyte concentration (or mass). The new ELS method works in pure DMSO.

The best current work-around is not to do size separation at all, but to determine the weight-average molecular weight and *z*-average radius of gyration of the unseparated sample using multiple-angle laser light scattering. The technique requires considerable care to produce valid data, and of course these average values do not provide as much information as their size distribution would.

The data from these various techniques have been used extensively in the literature. There are many papers deducing useful structure–property relations using the simplest level-1 structural parameter, the amylose fraction; many of these papers put forward plausible mechanistic reasons for the observed correlations. A more sophisticated approach is to consider not just simply amylose, but the amount of longer chains, whether from amylose or longer amylopectin branches; there are especially useful correlations with slow digestibility/highly resistant starch, explained in terms of retrogradation forming an enzyme-resistant crystalline structure after some or all branches are stripped from these longer branches during digestion.

The full CLD provides more extensive level 1 data. The commonest means of obtaining biosynthesis–structure–property relations from these data, which has produced much useful knowledge, is by parameterizing the CLD by an empirical division into various DP ranges, and then comparing across varieties (or species), often as difference plots. A new approach uses instead a biosynthesis-based parameterization of the full amylopectin CLD, which accurately represents this CLD in terms of a small number of parameters, readily obtained from experiment using publicly available code. This new method has already shown considerable promise in obtaining mechanistically reasonable and practically useful biosynthesis–structure–property relations.

At present, relatively limited use is made of the structural information available at level 2, viz., the fully branched, molecularly dispersed molecules. There are quite a few papers on structure–property relationships using $\overline{M}_{\mathrm{w}}$, but as stated, conclusions obtained with such data need to be treated circumspectly, because they are prone to experimental artifacts, especially if derived from SEC (because of shear scission). Two examples where size distributions have been used reliably to find useful information are as follows. (a) Changes in weight distributions during in vivo and in vitro digestion of starch leading to understanding of how resistant starch is formed, and (b) the discovery of differences in the size distributions of glycogen in a healthy and diabetic animal model, leading to a way to find new drug targets for diabetes management.

There is also the prospect of obtaining useful information from the level 2 size distributions of number of molecules (as distinct from the weight), $\overline{M}_{\mathrm{w}}$ and $\overline{M}_{\mathrm{n}}$. Such data can be obtained with present techniques (taking appropriate account of the problems and limitations discussed above) but have not been used to any real extent in the literature. For example, the number distribution of fully branched polysaccharides has considerable potential to unveil new knowledge of the biosynthetic mechanisms which formed the polymers, as has been done in the past with synthetic polymers (e.g., [92]).

Although there are real challenges with various unsolved or partially solved technical problems, the rewards from making full use of the information that can be obtained from multiple-level structural characterization of starch and glycogen are considerable with regard to human health (especially diabetes, obesity, and colorectal cancers) and learning more about the biosynthetic processes which produce most of our food energy.

Acknowledgements We gratefully acknowledge the support of ACW and MAS by Australian Postgraduate Award (APA) and Commonwealth Scientific and Industrial Research Organisation (CSIRO) Food Futures Flagship Scholarships and support of Australian Research Council grant LP0990769. We also acknowledge Mr. Torsten Witt for useful discussions, Ms. Ming Li for providing the extruded starch samples, and Dr. Kim Bell-Anderson (University of Sydney) for providing the samples for healthy mice data plotted in Fig. 3.

References

1. Byrnes SE, Miller JCB, Denyer GS (1995) J Nutr 125:1430–1437
2. Lehmann U, Robin F (2007) Trends Food Sci Technol 18:346–355
3. Johnston KL, Thomas EL, Bell JD, Frost GS, Robertson MD (2010) Diabet Med 27:391–397
4. Sullivan MA, Li J, Li C, Vilaplana F, Zheng L, Stapleton D, Gray-Weale AA, Bowen S, Gilbert RG (2011) Biomacromolecules 12:1983–1986
5. Gilbert RG (2011) Anal Bioanal Chem 399:1425–1438
6. Gilbert RG, Witt T, Hasjim J (2013) Cereal Chem. doi: 10.1094/CCHEM-1011-1012-0141-FI
7. Lopez-Rubio A, Flanagan BM, Gilbert EP, Gidley MJ (2008) Biopolymers 89:761–768
8. Morrison WR, Law RV, Snape CE (1993) J Cereal Sci 18:107–109
9. Sullivan MA, O'Connor MJ, Umana F, Roura E, Jack K, Stapleton DI, Gilbert RG (2012) Biomacromolecules 13:3805–3813
10. Perez S, Bertoft E (2010) Starch 62:389–420
11. Oostergetel GT, van Bruggen EFJ (1993) Carbohydr Polym 21:7–12
12. Gallant DJ, Bouchet B, Baldwin PM (1997) Carbohydr Polym 32:177–191
13. Jane J, Chen YY, Lee LF, McPherson AE, Wong KS, Radosavljevic M, Kasemsuwan T (1999) Cereal Chem 76:629–637
14. Dhital S, Shrestha AK, Gidley MJ (2010) Food Hydrocoll 24:152–163
15. Englyst HN, Kingman SM, Cummings JH (1992) Eur J Clin Nutr 46(Suppl 2):S33–50
16. Srichuwong S, Sunarti TC, Mishima T, Isono N, Hisamatsu M (2005) Carbohydr Polym 60:529–538
17. Chavez-Murillo CE, Mendez-Montealvo G, Wang YJ, Bello-Perez LA (2012) Starch 64:745–756
18. Zhu L-J, Liu Q-Q, Wilson JD, Gu M-H, Shi Y-C (2011) Carbohydr Polym 86:1751–1759

19. Hasjim J, Lee S-O, Hendrich S, Setiawan S, Ai Y, Jane J-L (2010) Cereal Chem 87:257–262
20. Cui R, Oates CG (1999) Food Chem 65:417–425
21. Gidley MJ, Cooke D, Darke AH, Hoffmann RA, Russell AL, Greenwell P (1995) Carbohydr Polym 28:23–31
22. Morell MK, Samuel MS, O'Shea MG (1998) Electrophoresis 19:2603–2611
23. O'Shea MG, Samuel MS, Konik CM, Morell MK (1998) Carbohydr Res 307:1–12
24. Wong KS, Jane J (1995) J Liq Chromatogr 18:63–80
25. Hanashiro I, Abe J, Hizukuri S (1996) Carbohydr Res 283:151–159
26. Wong KS, Jane J (1997) J Liq Chromatogr Relat Technol 20:297–310
27. Vilaplana F, Gilbert RG (2010) J Separation Sci 33:3537–3554
28. Baumgarten JL, Busnel JP, Meira GR (2002) J Liq Chromatogr Relat Technol 25:1967–2001
29. Castro JV, Ward RM, Gilbert RG, Fitzgerald MA (2005) Biomacromolecules 6:2260–2270
30. Konkolewicz D, Taylor JW II, Castignolles P, Gray-Weale AA, Gilbert RG (2007) Macromolecules 40:3477–3487
31. Vilaplana F, Hasjim J, Gilbert RG (2012) Carbohydr Polym 88:103–111
32. Gidley MJ (1985) Carbohydr Res 139:85–93
33. Tizzotti MJ, Sweedman MC, Tang D, Schaeffer C, Gilbert RG (2011) J Agric Food Chem 59:6313–6319
34. Zang LH, Rothman DL, Shulman RG (1990) Proc Natl Acad Sci U S A 87:1678–1680
35. Giddings JC (1993) Science 260:1456–1465
36. Striegel AM, Brewer AK (2012) Annu Rev Anal Chem 5:15–34
37. Grubisic Z, Rempp P, Benoit H (1967) J Polym Sci Polym Lett Ed 5:753–759
38. Kostanski LK, Keller DM, Hamielec AE (2004) J Biochem Biophys Methods 58:159–186
39. Goldwasser JM (1993) In: Provder T (ed) Absolute Mn determined by gel permeation chromatography—differential viscometry. Washington DC, ACS
40. Gray-Weale A, Gilbert RG (2009) J Polym Sci Part A Polymer Chem Ed 47:3914–3930
41. Jones RG, Kahovec J, Stepto R, Wilks ES, Hess M, Kitayama T, Metanomski WV (2009) Compendium of polymer terminology and nomenclature. IUPAC recommendations 2008. Royal Society of Chemistry, Cambridge
42. Schmitz S, Dona AC, Castignolles P, Gilbert RG, Gaborieau M (2009) Macromol Biosci 9:506–514
43. Syahariza ZA, Li E, Hasjim J (2010) Carbohydr Polym 82:14–20
44. Rolland-Sabaté A, Guilois S, Jaillais B, Colonna P (2011) Anal Bioanal Chem 399:1493–1505
45. Gidley MJ, Hanashiro I, Hani NM, Hill SE, Huber A, Jane J-L, Liu Q, Morris GA, Rolland-Sabaté A, Striegel A, Gilbert RG (2010) Carbohydr Polym 79:255–261
46. Ryu J-H, Drain J, Kim JH, McGee S, Gray-Weale A, Waddington L, Parker GJ, Hargreaves M, Yoo S-H, Stapleton D (2009) Int J Biol Macromol 45:478–482
47. Cave RA, Seabrook SA, Gidley MJ, Gilbert RG (2009) Biomacromolecules 10:2245–2253
48. Klavons JA, Dintzis FR, Millard MM (1997) Cereal Chem 74:832–836
49. Vilaplana F, Gilbert RG (2010) Macromolecules 43:7321–7329
50. Vilaplana F, Gilbert RG (2011) J Chromatogr A 1218:4434–4444
51. Juliano BO, Perez CM, Blakeney AB, Castillo T, Kongseree N, Laignelet B, Lapis ET, Murty VVS, Paule CM, Webb BD (1981) Starch 33:157–162
52. Mestres C, Matencio F, Pons B, Yajid M, Fliedel G (1996) Starch 48:2–6
53. Gibson TS, Solah VA, McCleary BV (1997) J Cereal Sci 25:111–119
54. Sullivan MA, Vilaplana F, Cave RA, Stapleton DI, Gray-Weale AA, Gilbert RG (2010) Biomacromolecules 11:1094–1100
55. Witt T, Doutch J, Gilbert EP, Gilbert RG (2012) Biomacromolecules 13:4273–4282
56. Syahariza ZA, Sar S, Tizzotti M, Hasjim J, Gilbert RG (2013) Food Chem 136:742–749
57. Ward RM, Gao Q, de Bruyn H, Gilbert RG, Fitzgerald MA (2006) Biomacromolecules 7:866–876
58. Wu AC, Gilbert RG (2010) Biomacromolecules 11:3539–3547
59. Wu AC, Morell MK, Gilbert RG (2013) PLoS ONE. doi: 10.1371/journal.pone.0065768
60. Wu AC, Gilbert RG (2013) Program "APCLDFIT". https://sourceforge.net/projects/starchcldfit/?source=directory
61. Nilsson L (2013) Food Hydrocoll 30:1–11
62. Periago MJ, Englyst HN, Hudson GJ (1996) Food Sci Technol 29:33–40
63. Woo KS, Seib PA (2002) Cereal Chem 79:819–825
64. Chung HJ, Liu Q, Hoover R (2010) Food Res Int 43:501–508
65. Zhang G, Ao Z, Hamaker BR (2008) J Agric Food Chem 56:4686–4694
66. Benmoussa M, Moldenhauer KAK, Hamaker BR (2007) J Agric Food Chem 55:1475–1479
67. Shin SI, Choi HJ, Chung KM, Hamaker BR, Park KH, Moon TW (2004) Cereal Chem 81:404–408
68. Chung HJ, Liu Q, Hoover R (2009) Carbohydr Polym 75:436–447
69. Shin SI, Kim HJ, Ha HJ, Lee SH, Moon TW (2005) Starch 57:421–430
70. Cai L, Shi Y-C (2010) Carbohydr Polym 79:1117–1123
71. Cai L, Shi Y-C, Rong L, Hsiao BS (2010) Carbohydr Polym 81:385–393
72. Witt T, Gidley MJ, Gilbert RG (2010) J Agric Food Chem 58:8444–8452
73. Jane J-L, Robyt JF (1984) Carbohydr Res 132:105–118
74. Hasjim J, Cesbron-Lavau G, Gidley MJ, Gilbert RG (2010) Biomacromolecules 11:3600–3608
75. Zhang G, Ao Z, Hamaker BR (2006) Biomacromolecules 7:3252–3258
76. Roesler WJ, Khandelwal RL (1985) Diabetes 34:395–402
77. Sharma K, McCue P, Dunn SR (2003) Am J Physiol Renal Physiol 284:F1138–1144
78. Besford QA, Sullivan MA, Zheng L, Gilbert RG, Stapleton D, Gray-Weale A (2012) Int J Biol Macromolecules 51:887–891
79. Chen H, Charlat O, Tartaglia LA, Woolf EA, Weng X, Ellis SJ, Lakey ND, Culpepper J, Moore KJ, Breitbart RE, Duyk GM, Tepper RI, Morgenstern JP (1996) Cell 84:491–495
80. Roesler WJ, Khandelwal RL (1986) Diabetes 35:210–216
81. Orrell SA, Bueding E (1964) J Biol Chem 239:4021–4026
82. Manners DJ (1991) Carbohydr Polym 16:37–82
83. Matsuda K, Hata K (1985) Denpun Kagaku 32:118–127
84. Drochmans P (1962) J Ultrastructural Res 6:141–163
85. Mordoh J, Krisman CR, Leloir LF (1966) Arch Biochem Biophys 113:265–&
86. Downs F, Pigman W (1970) Int J Protein Res 2:27
87. Radzicka A, Wolfenden R (1996) J Am Chem Soc 118:6105–6109
88. Copeland RA, Harpel MR, Tummino PJ (2007) Expert Opin Ther Targets 11:967–978
89. Hopkins AL, Groom CR (2002) Nat Rev Drug Discov 1:727–730
90. Gilbert RG, Besnard DJY, Reeve AJ, Lambides CJ, Hasjim J (2013) Starch. doi: 10.1002/star.201200257
91. Li E, Hasjim J, Singh V, Tizzotti M, Godwin ID, Gilbert RG (2013) Cereal Chem 90:223–230
92. Christie DI, Gilbert RG, Congalidis JP, Richards JR, McMinn JH (2001) Macromolecules 34:5158–5168